PHYSICAL REVIEW C VOLUME 8, NUMBER 5 NOVEMBER 1973

Coupled-Channel-Born-Approximation Analysis of One-Nucleon Transfer Reactions to ^{25}Mg and ^{25}Al

A. K. Abdallah and T. Udagawa
*Center for Nuclear Studies, University of Texas, Austin, Texas 78712**

and

T. Tamura
*Argonne National Laboratory, Argonne, Illinois 60439, and Center for Nuclear Studies, University of Texas, Austin, Texas 78712**

(Received 6 April 1973)

A simple formulation of the coupled-channel Born approximation is presented, for the case where the spin-dependent term in the optical potential can be ignored. The formalism is particularly useful in reducing the computer time required when numerical calculations are carried out for one-particle transfer reactions.

The formalism is then applied to calculate one-particle pickup and stripping reactions such as (p,d), $(^3\mathrm{He},\alpha)$, (d,t), and $(^3\mathrm{He},d)$, all leading to the 1.61-MeV $\frac{7}{2}^+$ and the 3.4-MeV $\frac{9}{2}^+$ states, together with the $\frac{5}{2}^+$ ground states in mass-25 nuclei. It is shown that the observed cross sections are all well reproduced by the Coupled-Channel–Born-approximation calculations.

1. INTRODUCTION

Much interest has been concentrated on the excitation of the 1.61-MeV $\frac{7}{2}^+$ states in ^{25}Mg and ^{25}Al by means of one-particle pickup and stripping reactions.[1-8] Note that these reactions are almost completely forbidden on the basis of a direct single-step mechanism, since the admixture of the $g_{7/2}$ single-particle state into the initial- and final-state wave functions is extremely small,[1] while experimentally observed cross sections are almost two orders of magnitude greater than that resulting from the above simple theoretical estimate.[1-6] Further, the shape of the observed angular distributions is generally found to disagree with the distorted-wave Born-approximation (DWBA) prediction with $l=4$.[1-4]

These experimental facts seem to show that the $\frac{7}{2}^+$ state is primarily excited through processes other than those of the direct single-step type. Since the nuclei involved in the reactions are strongly deformed, it is quite natural to expect that the multistep processes involving the inelastic scattering in both the incident and exit channels play an important role. Studies along this line have actually been made recently, in which the (d,p) reaction data for $E_d=13.5$ MeV[7] and 10.1 MeV[8] were specifically analyzed in terms of the coupled-channel Born approximation (CCBA).[9,10] Unfortunately, the conclusions obtained in the two independent works[7,8] contradicted with each other; in Ref. 7, the observed data (at $E_d=13.5$ MeV) were well reproduced in the calculations, while in Ref. 8, it was not possible to reproduce the data ($E_d=10.1$ and 12.3 MeV). The failure of the later work, however, could be attributed to the fact that the deuteron energy with which the author is concerned is not sufficiently high so that the measured cross sections involve a large contribution from compound processes.[8] Indeed, (d,p) data taken at small intervals of deuteron energy ranging from 6 to 13 MeV exhibited a rather marked variation with the incident energy, though the excitation function became comparatively smooth near 13 MeV.[11]

In order to get a clearer answer to the question of whether the forbidden transition to the $\frac{7}{2}^+$ state is indeed explained in terms of the CCBA, we have undertaken a systematic analysis of various one-particle transfer reaction data.[12] Experimental data are available for reactions such as (p,d), $(^3\mathrm{He},\alpha)$, (d,t), and $(^3\mathrm{He},d)$,[1-4] and we analyzed all of these data. Our analysis further included another forbidden transition, to the $\frac{9}{2}^+$ state at 3.4 MeV.

One problem in the CCBA analysis is that the calculation requires a large amount of computer time, particularly when the particle (the projectile or the outgoing particle) has a nonzero spin. However, under circumstances, such as those here, in which the spin-orbit part of the optical potential can safely be ignored, one can assume in the major part of the calculations that the incoming or outgoing particle has a vanishing spin, and thus one can speed up the calculations greatly. In Sec. 2, we thus present the reformulation of CCBA needed in carrying out this type of calculation.

Numerical results obtained by using the computer program MARS[13] are given in Secs. 3 and 4. In Sec. 3, the calculations are made of the ground $\frac{5}{2}^+$

and the 1.61-MeV $\frac{7}{2}^+$ cross sections, considering the 0^+ and 2^+ state coupling in the initial channel and also the $\frac{5}{2}^+$ and $\frac{7}{2}^+$ state coupling in the exit channel in generating the coupled-channel (CC) distorted waves,[14] while in Sec. 4, calculations are made of $\frac{9}{2}^+$ cross sections. Concluding remarks are given in Sec. 5.

2. FORMULATION OF CALCULATIONS

The reaction that is considered in the present work may be denoted as

$$a+A \to a+A' \to b+B' \to b+B, \tag{1}$$

where the first step, $a+A \to a+A'$, describes the elastic and inelastic scattering processes in the incident channels, characterized by a mass partition into the projectile a and the target A. The notation A' symbolizes excited states of A, though often where no confusion can arise it is understood to stand also for the ground state. The second step in Eq. (1), i.e., $a+A' \to b+B'$, describes the transfer processes and the third, $b+B' \to b+B$, the inelastic scattering processes in the exit channels that are characterized by a mass partition into the outgoing particle b and the residual nucleus B. The meaning of B' parallels that of A'.

The differential cross section of the above reaction processes can be written with the obvious notation as

$$\frac{d\sigma}{d\Omega} = [\mu_a\mu_b/(2\pi\hbar^2)^2](k_b/k_a)[1/(2I_A+1)(2s_a+1)] \times \sum_{m_a m_b M_A M_B} |T^{\mathrm{CCBA}}_{bBm_bM_B,\,aAm_aM_A}|^2, \tag{2}$$

where $T^{\mathrm{CCBA}}_{bBm_bM_BaAm_aM_A}$ is the transition amplitude in CCBA that we want to evaluate below.

To derive T^{CCBA}, let us first note that it is obtainable from the DWBA amplitude by replacing the elastically scattered distorted wave by a more general CC distorted wave,[14] which includes the inelastic scattering processes as well as the elastic. We denote such a generalized CC distorted wave by $\chi^{(\pm)}_{\alpha',\alpha}$, which describes the scattering state in the channel $\alpha' = (a'A'm_{a'}M_{A'})$ produced by the incident wave coming from the channel $\alpha = (aAm_aM_A)$.

With this generalized distorted wave, the total wave functions, $\Psi^{(+)}_\alpha$ and $\Psi^{(-)}_\beta$, of the incident and final channels with, respectively, the outgoing and incoming boundary condition, are given as

$$\Psi^{(+)}_\alpha = \sum_{\alpha'} \chi^{(+)}_{\alpha',\alpha}(\vec{k}_\alpha, \vec{r}_\alpha)\,|\,a'A'm_{a'}M_{A'}\rangle, \tag{3a}$$

$$\Psi^{(-)}_\beta = \sum_{\beta'} \chi^{(-)}_{\beta',\beta}(\vec{k}_\beta, \vec{r}_\beta)\,|\,b'B'm_{b'}M_{B'}\rangle. \tag{3b}$$

Note that $\chi^{(+)}_{\beta',\beta}$ and $\chi^{(-)}_{\beta',\beta}$ are related to one another through the time reversal relation given by

$$\chi^{(-)*}_{\beta',\beta}(\vec{k}_\beta, \vec{r}_\beta) = S_{\beta',\beta}\chi^{(+)}_{-\beta',-\beta}(-\vec{k}_\beta, \vec{r}_\beta), \tag{4a}$$

where

$$S_{\beta',\beta} \equiv (-)^{I_{B'}-I_B+M_{B'}+m_{b'}-M_B-m_b} \tag{4b}$$

and

$$-\beta \equiv (bB - m_b - M_B). \tag{4c}$$

In order to establish the partial-wave expansion of the distorted wave, for example $\chi^{(+)}_{\alpha',\alpha}$, let us first note that $\Psi^{(+)}_\alpha$ can also be rewritten as

$$\Psi^{(+)}_\alpha = \sum_{J_a l_{a'} A' m_{a'}} r_\alpha^{-1}\chi^{J_a}_{l_{a'},A'}(r_\alpha)\,|\,\Phi^{J_aM_a}_{l_{a'},A',s_am_a}\rangle, \tag{5}$$

where $|\,\Phi^{J_aM_a}_{l_{a'},A',s_am_a}\rangle$ is the channel wave function defined with standard notation by

$$|\,\Phi^{J_aM_a}_{l_{a'},A',s_am_a}\rangle = \sum \langle l_{a'}m_{l_{a'}}, I_{A'}M_{A'}|J_aM_a\rangle i^{l_{a'}} \times Y_{l_{a'}m_{l_{a'}}}\phi_{J_{A'}M_{A'}}\phi_{s_am_{a'}}. \tag{6}$$

We deliberately leave the spin of the incident particle uncoupled to the orbital angular momentum, since in the present approximation the spin-dependent term in the optical potential is ignored, and the spin of the incident particle plays no dynamical role during the scattering processes. It thus can be neglected in generating the CC distorted waves. This enables us to reduce the number of partial waves that are considered in solving the CC equations.

Inserting Eq. (6) into Eq. (5), we get

$$\Psi^{(+)}_\alpha = \sum_{\alpha' J_a l_{a'} m_{l_{a'}}} i^{l_{a'}} r_\alpha^{-1}\langle l_\alpha, m_{l_{a'}}, J_{A'}M_{A'}|J_aM_a\rangle\chi^{J_a}_{l_{a'},A'}Y_{l_{a'}m_{l_{a'}}}|\,a'A'm_{a'}M_{A'}\rangle. \tag{7}$$

Now, the partial wave amplitude, $\chi^{J_a}_{l_{a'},A'}$, in the above equation can further be written as a sum of partial-wave amplitudes, $\chi^{J_a}_{l_{a'},A',l_aA}$, which are those generated by an incident partial wave $(l_aAm_{l_a}M_A)$. Thus, one can write

$$\chi^{J_a}_{l_{a'},A'} = \sum_{l_am_{l_a}} \frac{4\pi}{k_\alpha}\hat{l}_a^{-1}\langle l_am_{l_a}J_AM_A|J_aM_a\rangle Y^*_{l_am_{l_a}}(\hat{k}_\alpha)\chi^{J_a}_{l_{a'},A',l_aA}, \tag{8}$$

where $\hat{l}\equiv\sqrt{2l+1}$ and the coefficient $4\pi/k_\alpha\langle l_a m_{l_a} I_A M_A | J_a M_a\rangle Y^*_{l_a m_{l_a}}(\hat{k}_\alpha)$ in Eq. (8) was introduced so that the boundary condition for $\chi^{J_a}_{l_a',A',l_aA}$ becomes simple, as is discussed for instance, in Ref. 14. Inserting Eq. (8) into Eq. (7) and comparing the resultant expression with Eq. (3a), one finds

$$\chi^{(+)}_{\alpha',\alpha}=\frac{4\pi}{k_\alpha r_\alpha}\sum_{J_a l_a l_a' m_{l_a} m_{l_a'}} i^{l_a'}\hat{l}_a^{-1}\chi^{J_a}_{l_a',A',l_aA}\langle l_a m_{l_a} I_A M_A | J_a M_a\rangle\langle l_a', m_{l_a'}, I_{A'} M_{A'} | J_a M_a\rangle Y^*_{l_a m_{l_a}}(\hat{k}_\alpha) Y_{l_a m_{l_a}}(\hat{r}_\alpha). \quad (10)$$

The CCBA transition amplitude can be expressed as

$$T^{\mathrm{CCBA}}_{\beta\alpha}=\langle\Psi^{(-)}_\beta | V | \Psi^{(+)}_\alpha\rangle$$
$$=\sum_{\alpha'\beta'}\iint d\vec{r}_\alpha d\vec{r}_\beta \chi^{(+)}_{-\beta'-\beta}(-\vec{k}_\beta,\vec{r}_\beta) S_{\beta'\beta}\langle b'B' m_{b'} M_{B'} | V | a'A' m_{a'} M_A\rangle \chi^{(+)}_{\alpha',\alpha}(\vec{k}_\alpha,\vec{r}_\alpha). \quad (11)$$

The interaction matrix element in Eq. (11) can be generally written as[15]

$$\langle bB m_b M_B | V | aA m_a M_A\rangle=\sum_{lsj} i^{-l} G^{BA}_{lsj m_l}(\vec{r}_\alpha,\vec{r}_\beta)\langle I_A M_A j m_j | I_B M_B\rangle(-)^{s_b-m_b}\langle s_a m_a s_b - m_b | s m_s\rangle\langle l m_l s m_s | j m_j\rangle. \quad (12)$$

Under the zero-range approximation, we have further[15]

$$G^{BA}_{lsj m_l}(\vec{r}_\alpha,\vec{r}_\beta)=D_0\hat{s}_a\alpha_{ba}A^{BA}_{lsj}F^{BA}_{lsj}(r_\alpha)Y^*_{l m_l}(\hat{r}_\alpha)\delta\left(\vec{r}_\beta-\frac{A}{B}\vec{r}_\alpha\right), \quad (13)$$

where D_0 is the zero-range parameter, α_{ba} the overlap of the spin-isospin wave functions of light projectile a and b, A^{BA}_{lsj} the spectroscopic amplitude, and $F^{BA}_{lsj}(r)$ the form factor, respectively.

Inserting Eqs. (10) and (12) into Eq. (11), and using Eq. (13), one can derive, after some manipulations, the following expression for the transition amplitude;

$$T^{\mathrm{CCBA}}_{bB m_b M_B, aA m_a M_A}=\sum_{lsj}\sum_{l_a l_b J_a J_b}\sum_{A' l_a' B' l_b'} D_0 A^{A'B'}_{lsj}\hat{s}_a\alpha_{ba}\Gamma^{lsj,J_aJ_b m,m_aM_Am_bM_B}_{l_aA,l_a'A',l_b'B',l_bB}P^m_{l_b}(\theta)I^{lsj,J_aJ_b}_{l_aA,l_a'A',l_b'B',l_bB}, \quad (14)$$

where Γ and I are, respectively, the angular momentum coupling coefficient and radial overlap integral given by

$$\Gamma^{lsj,J_aJ_b m,m_aM_Am_bM_B}_{l_aA,l_a'A',l_b'B',l_bB}=i^{l_a'+l_b'-l}\langle l_a' 0 l_b' 0 | l 0\rangle(-)^{s+l+I_{A'}-I_{B'}}\hat{l}_a'\hat{l}_b'\hat{J}_a\hat{J}_b\hat{j}\hat{s}^{-1}\hat{I}_{B'}\begin{pmatrix} l_a' & I_{A'} & J_a \\ l_b' & I_{B'} & J_b \\ l & j & s\end{pmatrix}$$
$$\times(-)^{(|m|-m)/2}\left[\frac{(l_b-|m|)!}{(l_b+|m|)!}\right]^{1/2}(-)^{l_b+m+I_B+M_B+s-m_s+s_b-m_b}$$
$$\times\langle l_a 0 I_A M_A | J_a M_A\rangle\langle J_a M_A J_b - m_s - M_A | s - m_s\rangle$$
$$\times\langle s_a m_a s_b - m_b | s m_s\rangle\langle l_b m I_B - M_B | J_b - m_s - M_A\rangle, \quad (15)$$

and

$$I^{lsj,J_aJ_b}_{l_aA,l_a'A',l_b'B',l_bB}=\frac{\sqrt{4\pi}}{k_a k_b}\frac{B}{A}\int\chi^{J_b}_{l_b'B',l_bB}\left(\frac{M_A}{M_B}r_a\right)F^{A'B'}_{lsj}(r_a)\chi^{J_a}_{l_a'A',l_aA}(r_a)dr_a. \quad (16)$$

$J_a(J_b)$ in the above equations stands for the total angular momentum of the orbital angular momentum $l_a(l_b)$ of the projectiles and the spin $I_A(I_B)$ of the nucleus;

$$\vec{J}_a=\vec{l}_a+\vec{I}_A \quad (\vec{J}_b=\vec{l}_b+\vec{I}_B). \quad (17)$$

Since the spin angular momentum of the projectiles is not included in the above total angular momentum $J_a(J_b)$, the latter is not conserved during the transfer processes. Actually, we have

$$\vec{J}_a=\vec{J}_b+\vec{s}. \quad (18)$$

For the case of $s=\frac{1}{2}$, this equation reduces to

$$J_a=J_b\pm\tfrac{1}{2}. \quad (19)$$

A computer program, MARS, has been written embodying the present CCBA formalism as a possible option for saving computer time.[13] MARS, however, can also perform the more general CCBA calculation, including the spin-dependent term in the optical potential. A final expression of the transition amplitude for such general CCBA calculations is also given in Ref. 13.

3. TRANSITIONS TO 1.61-MeV $\frac{7}{2}^+$ STATE

In this and the following sections, we discuss our analysis of experimental data for the following reactions: (p,d) with $E_p = 20$ MeV,[4] (^{3}He, α) with $E_h = 33$ MeV,[1] and (d,t) with $E_d = 21.5$ MeV[1] pickup reactions from ^{26}Mg target; and also (^{3}He, d) with $E_h = 20$ MeV,[3] stripping reactions from the ^{24}Mg target. The cross sections are calculated for the ground $\frac{5}{2}^+$, the 1.61-MeV $\frac{7}{2}^+$, and also the 3.4-MeV $\frac{9}{2}^+$ states of the final ^{25}Mg or ^{25}Al. These three states are known to be members of the $K = \frac{5}{2}^+$ rotational band associated with the [202] Nilsson single-particle state.[16] The target ^{26}Mg and ^{24}Mg are also known to be well deformed, the first excited 2^+ state of these nuclei being the 2^+ member of the $K = 0$ ground-state band. In the present section, we are concerned only with the $\frac{5}{2}^+$ and $\frac{7}{2}^+$ cross sections, considering the coupling between 0^+ and 2^+ states in the initial channel and $\frac{5}{2}^+$ and $\frac{7}{2}^+$ states in the final channel. The calculations of the $\frac{9}{2}^+$ cross section will be presented in the next section.

A. Form Factor and Optical Potential Parameters

In order to calculate the form factor, use is made of the Nilsson model. The spectroscopic amplitude corresponding to the transition from the initial spin I_i to the final spin I_f state is then given by[17]

$$A_{lsj}^{I_i \to I_f} = \hat{I}_f^{-1} \left\langle I_f \middle\| \begin{Bmatrix} a_{lsj} \\ a_{lsj}^\dagger \end{Bmatrix} \middle\| I_i \right\rangle = \hat{I}_i \hat{I}_f^{-1} \langle I_i 0\, j\tfrac{5}{2} | I_f \tfrac{5}{2} \rangle \sqrt{2} C_{jl} , \quad (20)$$

where C_{jl} is the Nilsson coefficient of the $K = \frac{5}{2}^+$ [202] orbit, (jl) specifying the basic spherical single-particle state. The radial wave function of the single-particle state (jl) then serves as the form factor of the transfer processes.

As is known,[1,16] the main component of the [202] $\frac{5}{2}^+$ Nilsson orbit is the $0d_{5/2}$ state. The mixing of the $0g_{7/2}$ and higher-spin states is extremely small. To illustrate this, we list in Table I the C_{jl}^2 values calculated by using the computer program NEPTUNE[18] which solves the coupled-channel equation for a nucleon bound in deformed Woods-Saxon potential. Three single-particle states, $d_{5/2}$, $g_{7/2}$, and $g_{9/2}$, are considered in the calculations, and as is seen the admixture of the $g_{7/2}$ and $g_{9/2}$ states into the $d_{5/2}$ state is indeed extremely small. This smallness of the mixing is the reason why the direct transitions to the $\frac{7}{2}^+$ and $\frac{9}{2}^+$ states are essentially forbidden. We thus neglect these small $\frac{7}{2}$ and $\frac{9}{2}$ form factors in the major part of the present calculations. Estimation of their effects will, nevertheless, be made later in Sec. 3 D.

TABLE I. C_{jl}^2 values of the Nilsson [202] $K = \frac{5}{2}^+$ orbit in ^{26}Mg. The values were calculated by solving the coupled-channel equation with a deformed Woods-Saxon potential. Parameters of the Woods-Saxon potential used in the calculation are: $a = 0.60$, $a_{so} = 0.65$, $r = 1.22$, $r_{so} = 1.27$, $V_{so} = 6.2$ MeV, and $\beta_2 = 0.40$; and the depth V of the potential needed to reproduce the experimental binding 11.01 MeV was found to be $V = 60.13$ MeV.

(lj)	$d_{5/2}$	$g_{7/2}$	$g_{9/2}$
C_{jl}^2	0.9788	0.0029	0.0183

The optical potential parameters used in the calculations and summarized in Table II were taken from literature, where the parameters were fixed from the optical-model analysis of the elastic scattering data (for ^{3}He and t)[1,19] or CC analysis of both elastic and inelastic scattering data (for p, d, and α).[6,20] Since we perform CCBA here, the parameters determined from the optical-model analysis, neglecting the inelastic coupling, should be renormalized so that the calculation including the inelastic coupling reproduces the elastic scattering as well as the inelastic scattering cross sections. In the present work, however, we used those parameters without such a renormalization. As is known,[14] however, the most important renormalization is to reduce the strength of the imaginary potential. We shall thus investigate later in Sec. 3 E the effect of reducing the imaginary potential on the transfer reaction cross sections, where the effects of the spin-orbit force which is neglected in the major part of the present calculations will also be discussed. In Table II, deformation parameters are also given, which are taken from the results of analysis of the inelastic scattering.[6,19,21] In Table III, we list the D_0^2 parameters [see Eq. (13)] assumed in the present calculations.[22]

B. Pickup Reactions

The results of the CCBA calculations for the pickup reactions are presented in Figs. 1(a)–1(c), and are compared with experiments. For the ground state, the DWBA cross sections are also presented. Note that the later (DWBA) cross sections are calculated by assuming the same optical potentials as those used in the CCBA calculations. This implies that though the inelastic couplings are neglected, the elastic distorting potentials are still generated from the deformed potential by making the Legendre expansion of the potential.[14] In each figure, an over-all normalization factor is introduced, which is fixed in such a way that the

TABLE II. Optical potential and deformation parameters used in the present calculations.

	V	W	W_D	a	a_I	a_D	r	r_I	r_D	r_C	β_2
p	46.0	0.0	10.0	0.60		0.64	1.22		1.27	1.22	
d	80.0	0.0	17.0	0.77		0.43	1.25		1.67	1.30	
t	142.3	23.5	0.0	0.695	0.80		1.22	1.506		1.30	
^{3}He	167.1	20.5	0.0	0.688	0.75		1.10	1.688		1.40	
α	171.0	19.0	0.0	0.55	0.52		1.53	1.53		1.53	
^{26}Mg											0.30
^{25}Mg and ^{25}Al											0.40
^{24}Mg											0.45

calculated CCBA ground-state cross section fits best the experimental data. The normalization factors thus determined are summarized in Table IV.

It is seen from the results that the observed cross sections are well reproduced in the calculations for both the $\frac{5}{2}^+$ and $\frac{7}{2}^+$ states. It is particularly remarkable that the $\frac{7}{2}^+$ cross section relative to that of $\frac{5}{2}^+$ is well explained in the calculations for all reactions considered.

The $\frac{7}{2}^+$ state may be excited through the inelastic scattering process in either the incident or the exit channel. In order to see the effect separately, we made another CCBA calculation, which includes only the $\frac{5}{2}^+$-$\frac{7}{2}^+$ coupling in the exit channel (i.e., neglects the incident 0^+-2^+ coupling in the incident channel). The resulting cross sections turned out to be smaller than those of Fig. 1 by about and only about a factor 2, systematically for all the reactions considered there. This result seems to show that the inelastic scattering effects in both channels are almost equally important, and also that both effects contribute coherently to the $\frac{7}{2}^+$ cross section.

It may also be interesting to note that we see in Fig. 1 rather large difference between the DWBA and CCBA cross sections for the unforbidden transition to the $\frac{5}{2}^+$ state, particularly in the (^{3}He, α) reaction. In this case, the CCBA cross section is larger by almost a factor 2 than that of DWBA. For other cases, the difference is less remarkable but still the CCBA cross section is larger, say, by about 20% than that of DWBA. These results show that the inelastic scattering processes can sometimes be very important for the nonforbidden transitions. It should be noted that for a deformed target with a spin I which is nonvanishing, an additional contribution takes place even if there is no coupling to other states. More specifically, for a fixed value J of the spin of the total system, several partial waves with total angular momentum $\vec{j} = \vec{J} - \vec{I}$ are coupled together, which causes the reorientation of the direction of the deformation axis in the process of the scattering. For the case of (^{3}He, α), for example, we made a calculation in which only the 0^+ state, was considered, and thus no coupling was allowed in the incident channel, while in the exit channel only the $\frac{5}{2}^+$ state was considered. Still the CCBA cross section differed from the DWBA cross section as much as factor 2 and was essentially the same as that of the full CCBA. This is probably a general result for large deformations.

The normalization factors that were introduced in Fig. 1 and tabulated in Table IV may be interpreted as a correction factor to the spectroscopic amplitude given in Eq. (20) and will describe the configuration mixing effects which are not accounted in deriving Eq. (20). As is seen, the correction factors agree with each other within 5%, implying that CCBA reproduces the absolute magnitude of the cross sections of various reactions consistently. On the other hand, in DWBA we get different values of spectroscopic factor for different types of reactions as already pointed out in Ref. 1. This discrepancy has now been removed in CCBA.

TABLE III. D_0^2 parameters used in the present calculations.

Reaction	D_0^2 (MeV^2 fm$^3\times 10^4$)
$\{(d,p)\}$ $\{(p,d)\}$	1.58
(^{3}He, α)	23.0
(d,t)	3.37
(^{3}He, d)	3.14

TABLE IV. Normalization factors introduced in obtaining the theoretical cross sections in Fig. 1.

Reaction	Normalization factor
(p,d)	0.80
(^{3}He, α)	0.82
(d,t)	0.84

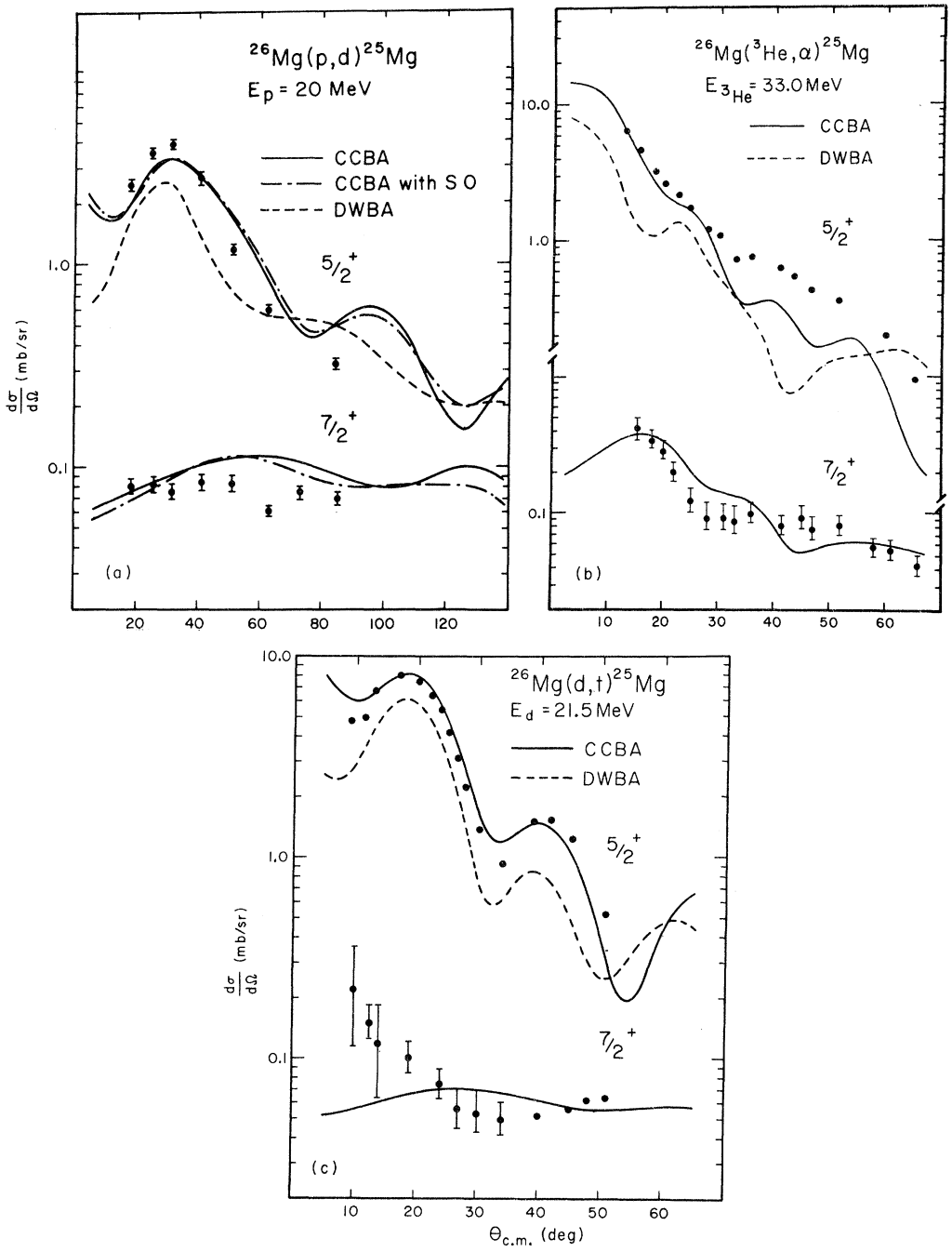

FIG. 1. (a) Cross sections for the ^{26}Mg$(p,d)^{25}$Mg reaction populating the $\frac{5}{2}^+$ ground and the $\frac{7}{2}^+$ 1.61-MeV state. The full curves are the CCBA cross sections and the dotted curve given for the $\frac{5}{2}^+$ state is the DWBA cross section. The DWBA cross section was calculated by using the same optical parameters as used for the CCBA calculations. The distortion effect of the optical potential due to the deformation is also included in the DWBA calculations by generating the potential in exactly the same way as we do in the CCBA. The data are taken from Ref. 4. The figure also includes a CCBA cross section obtained by taking into account the spin-orbit force of proton (V_{so}=6.2 MeV, r_{so}=1.22 fm, and a_{so}=0.60 fm). The discussion on the calculated cross section is given in Sec. 3 E. (b) Cross sections for the ^{26}Mg(^{3}He,α)^{25}Mg reaction populating the $\frac{5}{2}^+$ ground and the $\frac{7}{2}^+$ 1.61-MeV state. Other information is as given for (a), except that the data are taken from Ref. 1. (c) Cross sections for the ^{26}Mg$(d,t)^{25}$Mg reaction populating the $\frac{5}{2}^+$ ground and the $\frac{7}{2}^+$ 1.61-MeV state. Other information is as given for (a), except that the data are taken from Ref. 1.

C. Stripping Reactions

The results of the calculations for the (^{3}He, d) stripping reaction are presented in Fig. 2(a) and are compared with experiment.[3] No additional normalization factor was introduced in this case. As is seen, both the absolute magnitude and the shape of the observed cross sections are well explained by the calculations. It should be noted, however, that we observe a discrepancy at forward angles between the calculated and observed cross sections for the $\frac{7}{2}^+$ state; the experimental cross section increases with decreasing angle while the calculated cross section decreases. We have tried calculations with other sets of optical parameters, but so far we have not been able to reproduce the increase of the observed cross section at forward angles.

Besides the (^{3}He, d) data discussed above, (d, p) reaction data are also available which were, however, already analyzed[7,8] as was mentioned in the Introduction. We shall thus not repeat the analysis here. It should, however, be remarked here that there was an error in our previous calculation in Ref. 7, an error which fortunately did not affect seriously the final result. We present here in Fig. 2(b) the corrected results, together with the experimental data.[22]

D. Effects of the $\frac{9}{2}^+$ State and $g_{7/2}$ and $g_{9/2}$ Form Factors

So far we have neglected the $\frac{9}{2}^+$ state in obtaining the CC distorted wave in the final channel. The state is, however, coupled directly with the ground $\frac{5}{2}^+$ state, and thus we expect that the inclusion of this state affects the calculated cross sections. To

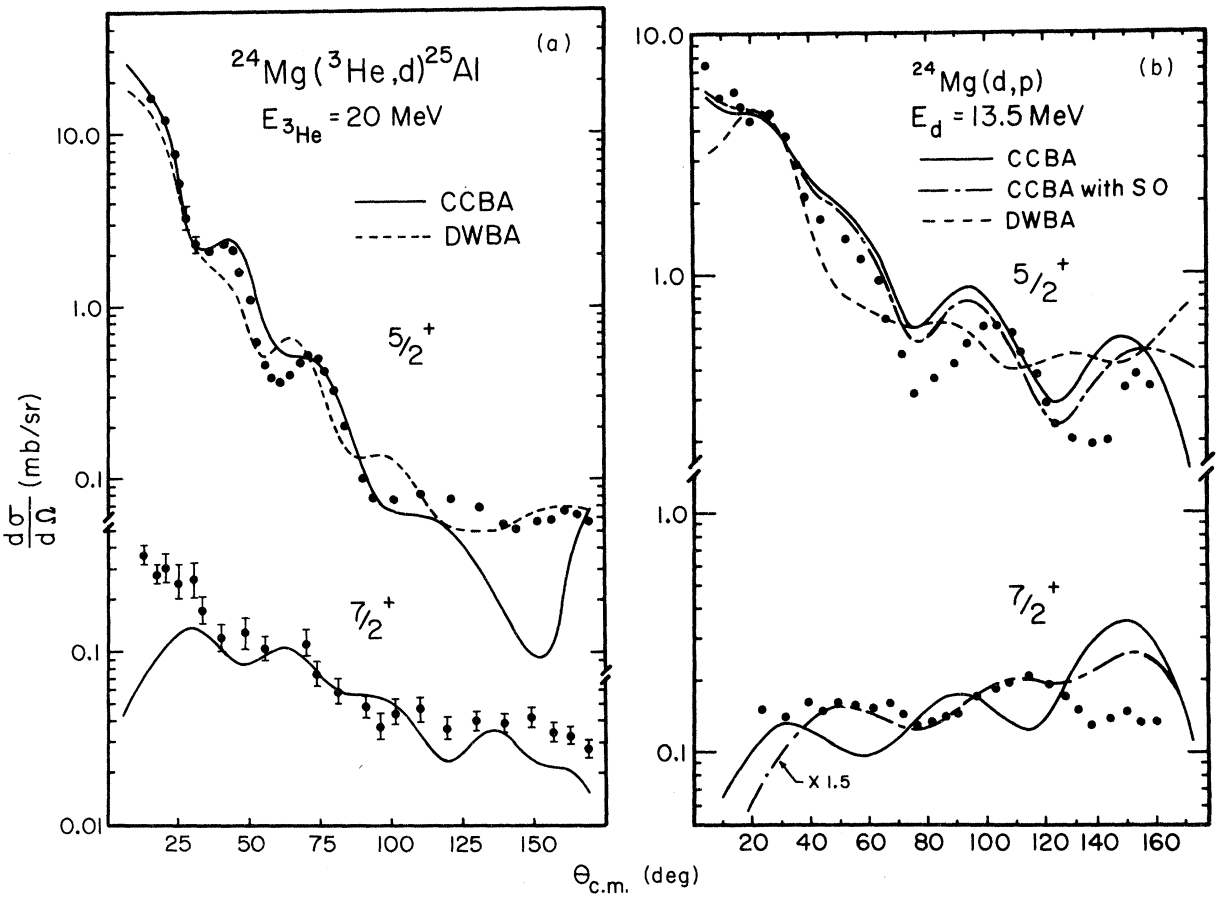

FIG. 2. (a) Cross sections for the ^{24}Mg(^{3}He,d)^{25}Al reaction populating the $\frac{5}{2}^+$ ground and the $\frac{7}{2}^+$ 1.61-MeV state. Other information is as given for Fig. 1(a), except that the data are taken from Ref. 3. (b) Cross section for the ^{24}Mg(d,p)^{25}Mg reaction populating the $\frac{5}{2}^+$ ground and the $\frac{7}{2}^+$ 1.61-MeV state. Other information is as given for Fig. 1(a), except that the data are taken from Ref. 6. The figure also includes a CCBA cross section obtained by taking into account the spin-orbit force of proton (V_{so} = 6.2 MeV, V_{so} = 1.22 fm, and a_{so} = 0.60 fm). The discussion on the calculated cross section is given in Sec. 3 E.

see the effects, we have actually performed calculations including the state for two examples of the reactions, (^{3}He, α) and (p,d). The results obtained are presented in Figs. 3(a) and 3(b) and are compared with the results already obtained before. From the comparison, it is seen that the inclusion of the $\frac{9}{2}^+$ state does not lead to any appreciable change in the final cross section.

We have also examined the effects of the $g_{7/2}$ and $g_{9/2}$ form factors by carrying out the calculations including both of them. The results obtained showed that the effects are not important for this case.

E. Effects of the Spin-Orbit Force and Other Choices of the Optical Parameters

In the calculations presented above we have ignored the spin-orbit force in the optical potential in order to make the numerical computation practically feasible, and with the belief that its effect is weak. As far as the α-particle channel is concerned, this of course does not mean any approximation. The approximation is expected to be good for the channels of ^{3}He and t, since the spin-orbit force for these particles is known to be small. The only cases where the spin-orbit force might produce an important effect would be those where protons and deuterons are involved in the reactions; indeed, in Ref. 8, the effect of the spin-orbit force was studied in (d,p) reaction case, showing that the proton spin-orbit force changes to some extent the angular pattern of the calculated CCBA cross section, though it does *not* affect the absolute magnitude. The effect of the deuteron spin-orbit force was also studied and it was found to be very small.

In order to see how significant is the effect of the spin-orbit force in our case, we also did a few additional calculations for (p,d) and (d,p) reactions, and the CCBA cross sections calculated by including the spin-orbit force in the proton channel are given in Figs. 1(a) and 2(b). As is seen in Fig. 1(a), the effect is rather small, only about 10%, for the (p,d) reaction. On the other hand, the effect is more significant for (d,p) reaction; the $\frac{7}{2}^+$ angular distribution is largely affected, the effect being, in our example, in such a way as to

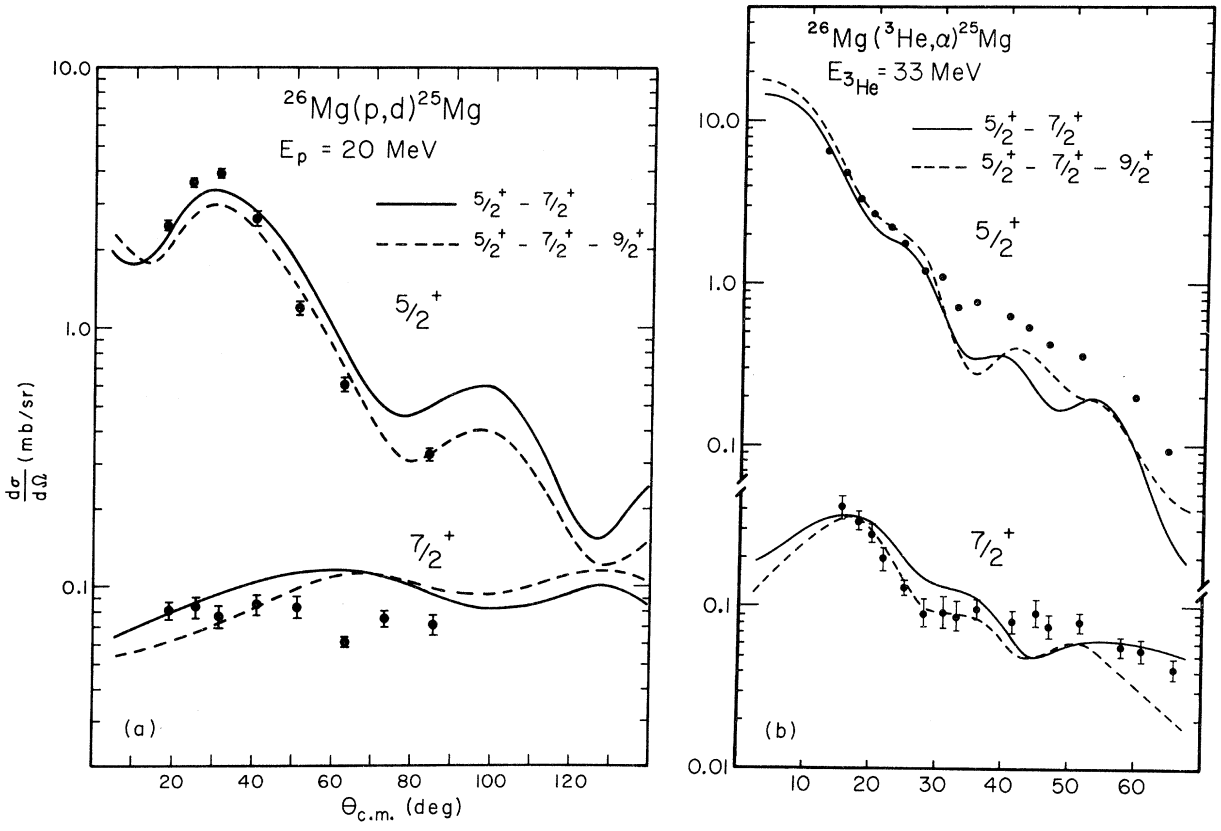

FIG. 3. (a) Comparison of the CCBA cross sections for the $\frac{5}{2}^+$ and $\frac{7}{2}^+$ states of the ^{26}Mg$(p,d)^{25}$Mg reaction obtained by including the $\frac{9}{2}^+$ state at 3.4 MeV in the CC calculations in the final channel with those obtained by excluding it. (b) Comparison of the CCBA cross sections for the $\frac{5}{2}^+$ and $\frac{7}{2}^+$ states of the ^{26}Mg(^{3}He,α)^{25}Mg reaction obtained by including the $\frac{9}{2}^+$ state at 3.4 MeV in the CC calculations in the final channel with those obtained by excluding it.

make the agreement with experiment much better than otherwise. The average absolute magnitude of the cross section is also slightly reduced (by about 20%).

As was already noted, use is made of the optical parameters for ^{3}He and t that were determined from the analysis neglecting the inelastic coupling. The use of these elastic parameters may not, however, be fully justified for the CCBA calculations which include the inelastic coupling explicitly. The most important renormalization of the parameters due to the inclusion of the inelastic coupling is a reduction of the imaginary part of the potential in the ground-state channel.[14] Our approximation to use the elastic parameters may thus be tested by redoing CCBA calculations by using a reduced imaginary strength of the potential in the ground channel, and then by comparing the results with those obtained previously. In addition to answering this specific question such calculations may also be of interest in order to see the sensitivity of the calculated cross sections on the optical parameters. With these considerations in mind, we performed calculations for (p,d) and $(^3\mathrm{He},\alpha)$ reactions by using the imaginary potentials whose strengths in the ground-state channel of both the target and residual nuclei were reduced by 20%.

The results of such calculations are given in Figs. 4(a) and 4(b) in comparison with the original results in Figs. 1(a) and 1(b). Note that in Fig. 4 we introduced spectroscopic factors which are smaller, respectively, by 30 and 20%, than those of Fig. 1 and tabulated in Table IV. This means that the newly calculated cross sections are larger by these amounts than those obtained before. Nevertheless, as is seen from the figure, the $\frac{7}{2}^+$ cross section relative to that of $\frac{5}{2}^+$ state remains almost unchanged. Similar results were also obtained for the cases where we reduce the imaginary potential in the ground channel of only the target or of the residual nucleus.

Besides the imaginary part of the optical poten-

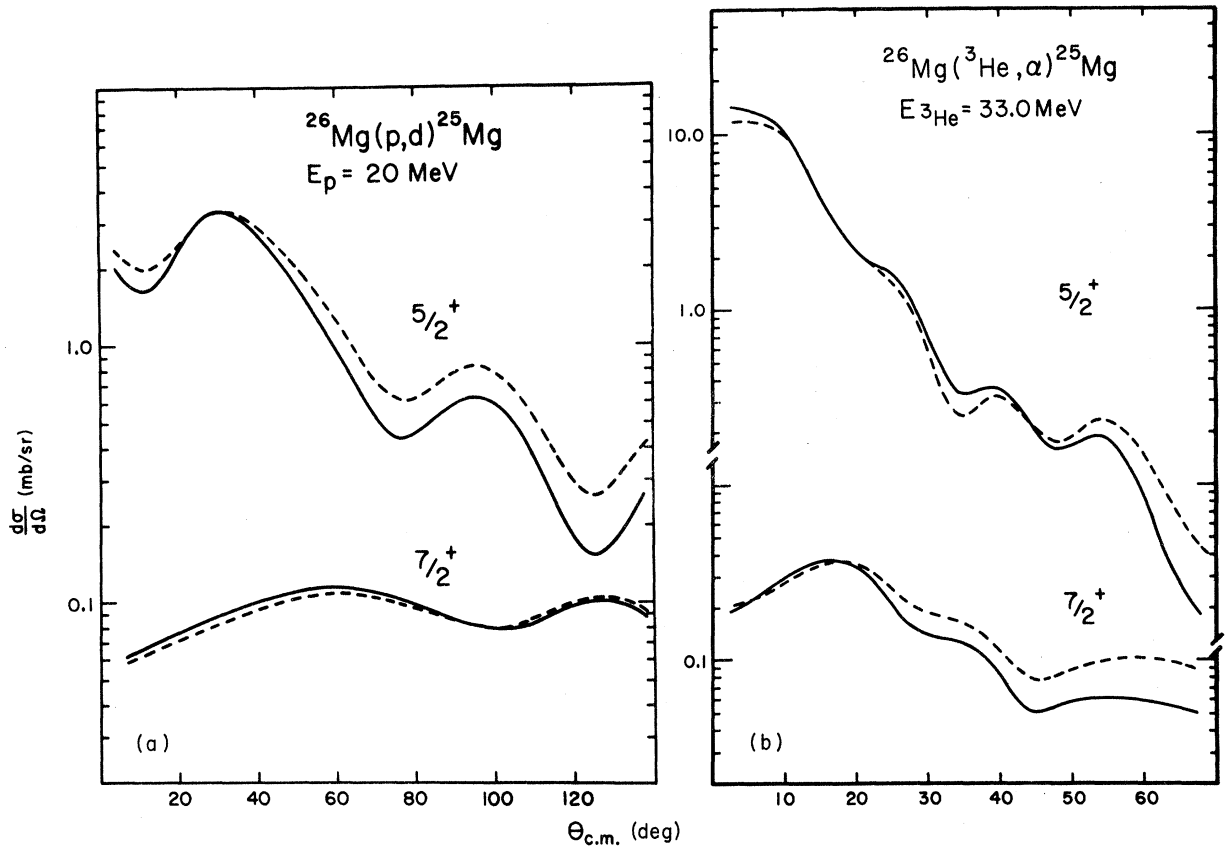

FIG. 4. (a) Comparison of the CCBA cross sections (broken line) for the $\frac{5}{2}^+$ and $\frac{7}{2}^+$ states of the ^{26}Mg$(p,d)^{25}$Mg reaction obtained by reducing the strength of the imaginary part of the optical potential in the ground-state channels of both the target and residual nuclei by 20% with those of Fig. 1(a) (full line). (b) Comparison of the CCBA cross sections (broken line) for the $\frac{5}{2}^+$ and $\frac{7}{2}^+$ states of the ^{26}Mg$(^3\mathrm{He},\alpha)^{25}$Mg reaction obtained by reducing the strength of the imaginary part of the optical potential in the ground-state channels of both the target and residual nuclei by 20% with those of Fig. 1(b) (full line).

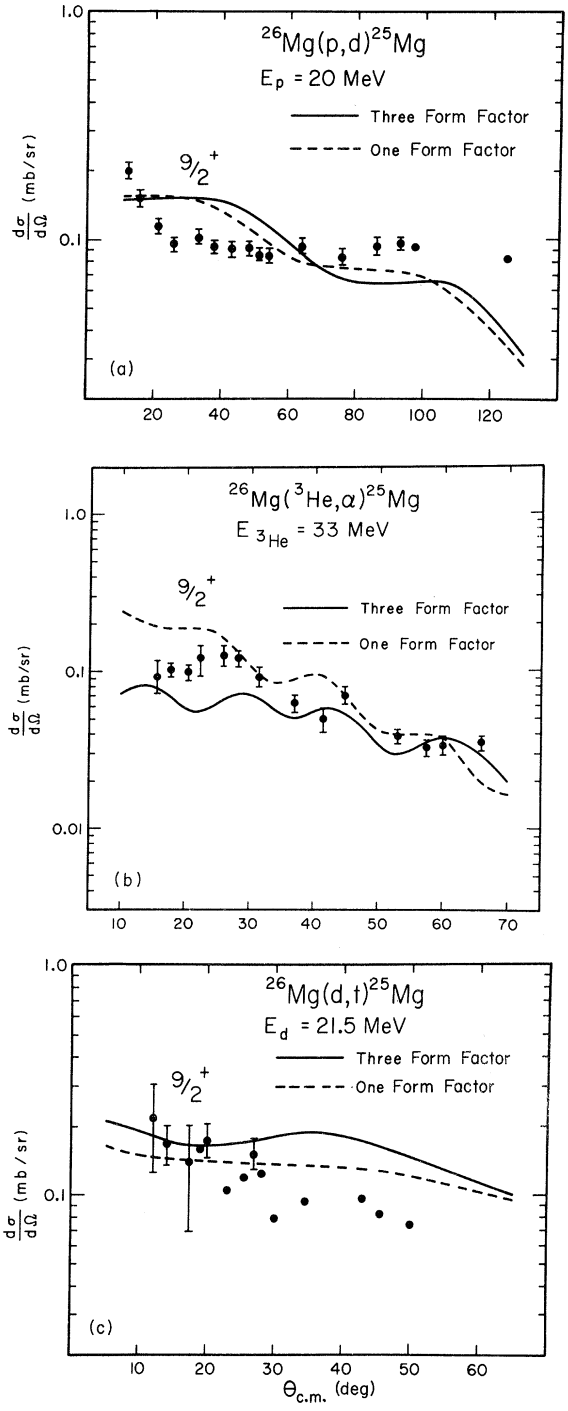

FIG. 5. (a) Comparison of the CCBA cross sections for the $\frac{9}{2}^+$ state of ^{26}Mg$(p,d)^{25}$Mg reaction with experiments. Two CCBA cross sections are given for each case, which are obtained by including and neglecting the $g_{7/2}$ and $g_{9/2}$ form factors. (b) Comparison of the CCBA cross sections for the $\frac{9}{2}^+$ state of ^{26}Mg$(^3\text{He},\alpha)^{25}$Mg reaction with experiments. (c) Comparison of the CCBA cross sections for the $\frac{9}{2}^+$ of ^{26}Mg$(d,t)^{25}$Mg reaction with experiments.

tial, we also examined the dependence of the cross section on a few other parameters, and found that the relative cross sections are quite insensitive, in general, to the choice of the parameters. We may thus state rather safely that the conclusions, we derived above through our CCBA calculation with a few simplifying assumptions, remain basically unaffected.

4. TRANSITIONS TO 3.4 MeV $\frac{9}{2}^+$ STATE

We now extend our analysis to another example of a forbidden transition, to the 3.4-MeV $\frac{9}{2}^+$ state. Since the actual data are available only for pickup reactions, the calculations are restricted to these reactions. The calculations are performed by considering the $\frac{5}{2}^+$, $\frac{7}{2}^+$, and $\frac{9}{2}^+$ states in the final channel, and also the $g_{7/2}$ and $g_{9/2}$ form factors, as in Sec. 3 D. For the purpose of comparison, however, calculations in which the $g_{7/2}$ and $g_{9/2}$ form factors are neglected are also made. The results obtained are summarized in Figs. 5(a)–5(c), together with the experimental cross sections. The same normalization factors as used in Fig. 1 were also consistently introduced here.

The results show that the observed cross sections are fairly well reproduced in the calculations. It is also seen that the calculated cross sections obtained by including the $g_{7/2}$ and $g_{9/2}$ form factors are not much different from those obtained by neglecting them. This implies that the major contribution to the $\frac{9}{2}^+$ cross section comes from the two-step processes, demonstrating again the importance of the inelastic scattering processes.

5. CONCLUDING REMARKS

An expression was derived for the CCBA transition amplitude, under the assumption that no spin-dependent term is present in the distorting optical potential. The derived expression, which allows to make CCBA calculation rather fast was then used to study the effects of the inelastic scattering processes on the forbidden transitions to the 1.61-MeV $\frac{7}{2}^+$ and the 3.4-MeV $\frac{9}{2}^+$ states in the mass 25 nuclei observed in (^{3}He, α), (p,d), (d,t), and (^{3}He, d) reactions. It is found that the observed cross sections to these states are well reproduced by the CCBA calculations. This shows that the forbidden transitions can indeed be explained in terms of the two-step processes via the inelastic scattering processes. Note that this conclusion is unchanged, as was discussed in Sec. 3 E, even when the spin-orbit interaction is included and thus full size CCBA calculations are made.

The inelastic scattering processes were found to play an important role also for some of the allowed

transitions. This was particularly demonstrated in the fact that the relative cross sections between various one-particle pickup reactions can be explained only when CCBA is used. DWBA does fail to explain them, as was pointed out earlier.[1]

Similar forbidden transitions to those discussed here are also expected to be observed in reactions involving other nuclei and also other states belonging to different rotational bands. The data would provide a further test of the CCBA calculations performed here and thus it would be interesting to extend the analysis if the data are accumulated.[12]

The authors wish to thank Professor W. R. Coker for a careful reading of the manuscript.

---

*Work supported in part by U. S. Atomic Energy Commission.

[1]D. Dehnhard and J. L. Yntema, Phys. Rev. 155, 1269 (1967); 160, 964 (1967).
[2]B. Cujec, Phys. Rev. 136, B1305 (1964).
[3]B. Mertens, C. Mayer-Boricke, and H. Kattenborn, Nucl. Phys. A158, 97 (1970).
[4]J. Kroon, R. Fournier, R. J. W. Hodgson, and B. Hird, Nucl. Phys. A172, 99 (1972).
[5]P. J. Iano and N. Austern, Phys. Rev. 151, 853 (1966).
[6]H. Schulz, H. J. Wiebicke, R. Fülle, D. Netzband, and K. Schlott, Nucl. Phys. A159, 324 (1970).
[7]D. Braunschweig, T. Tamura, and T. Udagawa, Phys. Lett. 35B, 273 (1971).
[8]R. S. Mackintosh, Nucl. Phys. A170, 353 (1971).
[9]S. K. Penny and G. R. Satchler, Nucl. Phys. 53, 145 (1964).
[10]R. J. Ascuitto and N. R. Glendenning, Phys. Rev. C 2, 1260 (1970).
[11]R. H. Siemssen and C. Mayer-Borick, private communication.
[12]Recently, CCBA analyses were made of the one-particle transfer reactions involving other nuclei than those considered here and were reported in R. O. Nelson and N. R. Roberson, Phys. Rev. C 6, 2153 (1972); P. J. Ellis and A. Dudek, to be published.
[13]T. Tamura and T. Udagawa, Center for Nuclear Studies, University of Texas, Technical Report No. 30, 1972 (unpublished).
[14]T. Tamura, Rev. Mod. Phys. 37, 679 (1965).
[15]G. R. Satchler, Nucl. Phys. 55, 1 (1964).
[16]B. R. Mottelson and S. G. Nilsson, K. Dan. Vidensk. Selsk. Mat.-Fys. Skr. 1, No. 8 (1959).
[17]G. R. Satchler, Ann. Phys. (N.Y.) 3, 275 (1957).
[18]T. Tamura, Center for Nuclear Studies, University of Texas, Technical Report No. 16, 1968 (unpublished).
[19]R. M. Drisko, P. G. Roos, and R. H. Bassel, J. Phys. Soc. Jap. Suppl. 24, 347 (1968).
[20]K. A. Eberhard and D. R. Robson, Phys. Rev. C 3, 149 (1971).
[21]R. De Swiniarski, C. Glashausser, D. L. Hendrie, J. Sherman, A. D. Bacher, and E. A. McClatchie, Phys. Rev. Lett. 23, 317 (1969); H. Rebel, G. W. Schweimer, G. Schatz, J. Specht, R. Lohken, G. Hausen, D. Hars, and H. Kewe-Nebenius, Nucl. Phys. A182, 145 (1972); P. L. Ottavani and L. Zuffi, *ibid.* A152, 570 (1970).
[22]R. H. Bassel, R. M. Drisko, and G. R. Satchler, Oak Ridge National Laboratory Report No. ORNL-3240 (unpublished); R. H. Bassel, Phys. Rev. 149, 791 (1966); R. Stock, R. Bock, P. David, H. H. Duhm, and T. Tamura, Nucl. Phys. A104, 136 (1967).
[23]Note also that in Ref. 7 the CC distorted waves were generated by assuming a real form factor for the coupling potential.